

$$\omega' = ku_0, \quad \omega'' = \frac{(\varepsilon+1)\omega_2^2}{8\pi\sigma_0} \frac{u-u_0}{u_0}. \quad (9)$$

The inequality $k^2 r_D^2 \ll k\Delta$ is easily compatible with the inequality $k\Delta \ll 1$ over a wide range of substrate carrier densities and temperatures. For $N_S \sim 10^8 \text{ cm}^{-2}$ and $\Delta \sim 10^{-5} \text{ cm}$, we obtain $u_0 \sim 10^6 \text{ cm/sec}$ for virtually all values of k (for which, of course, $k < N_S^{1/2}$). In connection with this estimate we note that the drift velocities in some semiconductors are much higher (e.g., $5 \times 10^7 \text{ cm/sec}$ in InSb).

¹As before, we assume the dielectric constant to be the same in all of space. No real difficulty is encountered in taking the differences in the values of ε in various regions into account, but the resulting formulas, although they are very cumbersome, do not alter the qualitative picture.

¹S. J. Allen Jr., D. C. Tsui, and R. A. Logan, Phys. Rev. Lett. 38, 980 (1977).

²T. N. Theis, J. P. Kotthaus, and P. J. Stiles, Solid State

Commun. 24, 273 (1977); 26, 603 (1978); Surf. Sci. 73, 434 (1978).

³D. C. Tsui, S. J. Allen Jr., R. A. Logan, A. Kamgar, and S. N. Coppersmith, Surf. Sci. 73, 419 (1978).

⁴T. N. Theis, Trans. Yamada Conf. II on Electronic properties of two-dimensional systems, Lake Yamanaka, Japan, 2-6 September 1979, p. 773.

⁵A. B. Mikhailovskii, Teoriya plazmennykh neustoičivostei (Theory of plasma instabilities), Atomizdat., 1977.

⁶A. B. Mikhailovskii and É. A. Pashitskii, Zh. Tekh. Fiz. 36, 1731 (1966) [Sov. Phys. Tech. Fiz. 11, 1291 (1967)].

⁷A. B. Mikhailovskii and É. A. Pashitskii, Zh. Eksp. Teor. Fiz. 48, 1787 (1965) [Sov. Phys. JETP 21, 1197 (1965)].

⁸L. L. Chang and L. Easaki, Trans. Yamada Conf. II on Electronic properties of two-dimensional systems, Lake Yamanaka, Japan, 2-6 September 1979, p. 17.

⁹R. Dingle, H. L. Störmer, A. C. Gossard, and W. Wiegmann, Trans. Yamada Conf. II on Electronic properties of two-dimensional systems, Lake Yamanaka, Japan, 2-6 September 1979, p. 30.

¹⁰M. V. Krashennnikov and A. V. Chaplik, Zh. Eksp. Teor. Fiz. 75, 1907 (1978) [Sov. Phys. JETP 48, 960 (1978)].

Translated by E. Brunner

Absorption of surface electromagnetic waves by thin oxide films on metal surfaces

G. N. Zhizhin, M. A. Moskaleva, E. I. Firsov, E. V. Shomina, and V. A. Yakovlev

Spectroscopy Institute, USSR Academy of Sciences

(Submitted 4 January 1980)

Zh. Eksp. Teor. Fiz. 79, 561-574 (August 1980)

The effect of thin silicon oxide films on the propagation of infrared surface electromagnetic waves (SEW) over copper is investigated. The SEW spectra are used to determine the optical constants of the films and substrates. The SEW spectra of natural oxide films on aluminum and on molybdenum are obtained.

PACS numbers: 78.20.Dj, 78.65.Jd, 73.40.Ns

Surface IR electromagnetic waves (SEW), which can propagate over the surface of a well-conducting metal to distances up to several centimeters,^{1,2} are very sensitive to the surface state of the metal and to the presence of thin films on the surface. The increase of the SEW absorption following the deposition of a film, with the absorption increasing near the film oscillation frequencies, permits the development of a new effective spectroscopic method—the spectroscopy of surface electromagnetic waves.^{2,3}

This method was used for an experimental investigation of silicon monoxide films on copper, of apatite on silver,⁴ and of films of cellulose acetate and benzene on copper.⁵ Investigation of the absorption of the SEW has made it possible to obtain a dependable spectrum of a monomolecular Langmuir film of siloxane acid on the surface of copper.⁶ The spectrum obtained by us earlier⁴ for the SEW of a silicon monoxide film on a copper surface differs noticeably from that calculated by using the published data on the optical constants of silicon monoxide.⁷ In the present paper we have used the SEW spectra to determine the optical constants of silicon-oxide films on copper surface and of the natural oxide

film on aluminum and molybdenum in the 10- μm region of the spectrum (CO₂ laser).

1. THEORY

Surface optical excitations exist on the interface of two media with dielectric constants ε that have opposite signs. Agranovich and Ginzburg² have developed the crystal optics of surface waves and have shown that, in analogy to three-dimensional crystal optics, the propagation of SEW can be described by introducing the SEW refractive index (which we designate by κx), which connects the frequency ν and the excitation wave vector k_x .¹⁻³ When damping is taken into account, the refractive index of SEW becomes complex, and its imaginary part defines the SEW absorption coefficient α . The reciprocal of the absorption coefficient is called the path length L (distance over which the SEW intensity attenuates by a factor $e = 2.72$).

Consider an air-metal interface. Air has $\varepsilon_1 = 1$; using for the metal the Drude formula for the dielectric constant, we obtain²

$$\alpha = 1/L \approx 2\pi\nu^2\nu_0/\nu_p^2, \quad (1)$$

where ν_p is the frequency of the plasma oscillations and ν_r is the frequency of the electron collisions. This formula is valid in the IR band at $\nu \ll \nu_p$. In the 10- μ m region of the spectrum, the absorption is small and the SEW path length can reach several centimeters.¹

If the metal surface is coated with a thin dielectric film, the calculation becomes much more complicated,³ since a complicated nonlinear equation must be solved. As shown by Agranovich and Ginzburg,² the presence of the surface layer (thin film) on the interface leads to resonances of the refractive index of the SEW at the frequencies of the transverse and longitudinal oscillations of the layer, i.e., to an increase of the SEW absorption coefficient at these frequencies. It can also be shown that for a film on a metal, the absorption in the IR region at the frequency of the transverse phonon is much weaker than at the frequency of the longitudinal phonon. Experiments have confirmed⁴ that the maximum SEW absorption is close to the frequency of the longitudinal oscillations of the film.

In the case of a film deposited on a metal surface, it must be taken into account that most metals are coated also by a natural oxide film several dozen angstrom thick. To obtain the dispersion equations with allowance for this film it is therefore necessary, when solving Maxwell's equations, to take into account boundary conditions on three boundaries of four media:

$$(\beta_1 + \beta_2)A + (\beta_1 - \beta_2)B e^{-2\kappa_2 d} = 0, \quad (2)$$

where

$$\begin{aligned} A &= (\beta_2 + \beta_3)(\beta_3 + \beta_1) + (\beta_2 - \beta_3)(\beta_3 - \beta_1) e^{-2\kappa_3 l}, \\ B &= (\beta_2 - \beta_3)(\beta_3 + \beta_1) + (\beta_2 + \beta_3)(\beta_3 - \beta_1) e^{-2\kappa_3 l}, \\ \beta_1 &= \epsilon_1 / \kappa_1, \quad \kappa_1 = [k_x^2 - \epsilon_1 (2\pi\nu)^2]^{1/2}, \end{aligned}$$

the media 1 (air) and 4 (metal) are semi-infinite, medium 2 is a film of thickness d , and medium 3 is the natural oxide film of thickness l . We note that if it is necessary to perform calculations for a large number of layers, then the recurrence formulas obtained in Ref. 8 can be used.

Formula (2) can be used only for computer calculations. To obtain an idea of the influence of the films on the SEW absorption, an approximate formula can be derived. If $\kappa_2 d \ll 1$, $\kappa_3 l \ll 1$, and $|\epsilon_4| \gg 1$, we obtain for the absorption coefficient

$$\begin{aligned} \alpha(\nu) \approx 2\pi\nu\epsilon_1^{1/2} & \left[\text{Im}(-1/\epsilon_1) + 4\pi\nu l \text{Im} \left(\frac{1 - \epsilon_1/\epsilon_3 - \epsilon_3/\epsilon_4}{(-\epsilon_1)^{1/2}} \right) \right. \\ & \left. + 4\pi\nu d \text{Im} \left(\frac{1 - \epsilon_1/\epsilon_2 - \epsilon_2/\epsilon_4}{(-\epsilon_1)^{1/2}} \right) \right]. \quad (3) \end{aligned}$$

Using the Drude model for the metal, we get

$$\begin{aligned} \alpha(\nu) \approx 2\pi\nu\epsilon_1^{1/2} & \left[\frac{\nu\nu_r}{\nu_p^2} + \frac{4\pi\nu^2 l}{\nu_p} \text{Im} \left\{ \left(1 + i \frac{\nu_r}{2\nu} \right)^{1/2} \left(1 - \frac{\epsilon_1}{\epsilon_3} - \frac{\epsilon_3}{\epsilon_4} \right) \right\} \right. \\ & \left. + \frac{4\pi\nu^2 d}{\nu_p} \text{Im} \left\{ \left(1 + i \frac{\nu_r}{2\nu} \right)^{1/2} \left(1 - \frac{\epsilon_1}{\epsilon_2} - \frac{\epsilon_2}{\epsilon_4} \right) \right\} \right]. \quad (4) \end{aligned}$$

Thus, the SEW absorption coefficient is proportional to the film thickness. The absorption is largest at the frequency at which $-\text{Im}(1/\epsilon)$ has a pole, i.e., at the frequency of the longitudinal oscillations of the film, while the second absorption maximum (at the frequency of the film transverse oscillations, the $\text{Im}\epsilon$ pole), is much smaller and is not observed in the experiment. The

SEW absorption by thin films is additive.

Qualitatively similar spectra are obtained by another method, used of late in the study of thin film on metal surfaces, namely by investigating the absorption produced upon reflection, from the sample, of light incident at a grazing angle θ and polarized in the incidence plane.⁹ The coefficient of the light reflection from the two films (d and l) on the metal surface is given by

$$R = \left| \frac{(\beta_1 - \beta_2)A + (\beta_1 + \beta_2)B \exp(-2\kappa_2 d)}{(\beta_1 + \beta_2)A + (\beta_1 - \beta_2)B \exp(-2\kappa_2 d)} \right|^2. \quad (5)$$

The notation is the same as in (2), and $k_x = 2\pi\nu\epsilon_1^{1/2} \sin\theta$. Just as for SEW, the absorption of the light (the decrease of the reflection) takes place predominantly at the frequencies of the longitudinal oscillations of the film. This method was used by us when it was necessary to obtain information on the spectrum of the investigated films in a wider frequency range than the tuning range of the CO₂ laser used to excite the SEW.

For an exact calculation of the SEW with the aid of the complete equation (5), a program was written for the solution of the complicated nonlinear equation by the method of steepest descent in the gradient direction. The reflection spectra were also calculated by computer.

2. SAMPLE PREPARATION

We investigated samples obtained by thermal evaporation in a vacuum of 10^{-6} – 10^{-5} Torr. To this end, a copper layer was first simultaneously deposited from a molybdenum vessel (or an aluminum layer from a tungsten coil) on three glass substrate plates measuring $130 \times 30 \times 6$ mm. The copper film was ~ 3000 Å thick, much thicker than the depth of penetration of the SEW field into the metal (several hundred angstroms). Calculation by formula (2) has shown that for copper films thicker than 1000 Å, on various substrates, the absorption is the same as for semi-infinite metal. We therefore neglect hereafter the finite thicknesses of the copper and aluminum films.

After exposing the entire length of the copper plate to air, silicon monoxide films were deposited on half the plate area from an evaporator made of molybdenum foil. Prior to the opening of the shutter, the rate of evaporation was set at ~ 5 Å/sec. The evaporated material was first deposited only on one substrate, and the other two were covered with a shield. The shield was next moved, and the film continued to be deposited on two substrates simultaneously; finally, the screen was completely removed and all three substrates were coated. This coating method gave grounds for expecting the obtained films not to differ greatly in composition and structure, compared with films obtained in different coating cycles. It must be noted that the films obtained by evaporation of silicon monoxide are very sensitive to the preparation conditions (evaporator temperature, rate of coating, oxygen pressure).¹⁰ Under conditions close to ours, the films produced are as a rule neither pure silicon monoxide nor silicon dioxide, but of intermediate composition [usually designated SiO_x ($1 \leq x \leq 2$)]. We shall therefore use the term silicon oxide rather than monoxide.

3. MEASUREMENT OF SEW SPECTRA

The experimental setup for the measurement of the SEW spectra is shown in Fig. 1. The radiation source 1 was a CO₂ laser (LG-22) operating in the single-mode regime. The exit mirror was replaced by diffraction grating 2 (100 lines/mm, blaze angle 30°), which made possible lasing on various rotational components of the vibrational bands of CO₂ in the 10-μm range. After reflection by mirrors 3 and 4 (which ensured constancy of the direction and prevented shifting of the beam when the grating was rotated), the laser beam was incident on a beam splitter 5 that diverted part of the energy into the working channel of the IR spectrophotometer IKS-16, for frequency calibration. The optical system was adjusted by He-Ne laser 6. Past the modulator 7, which chopped the radiation at a frequency 400 Hz, and past mirror 8, the laser beam was divided by beam splitter 9 (sodium-chloride plate) into two beams: a comparison beam that monitored the stability of the laser radiation, and a working beam containing the measuring pickup with the investigated sample.

The excitation of the SEW and the reconversion of the surface wave into a volume wave were effected by potassium bromide or sodium chloride prisms.¹⁻⁶ The prisms and the sample were placed in a measuring pickup that allowed adjustment of the gaps between the prisms and the sample, as well as of the angle of incidence of the light in the prism, to optimize the SEW excitation conditions.¹¹ The beam past the exit prism was focused by sodium-chloride lens 11 on the radiation receiver 12, whose signal was amplified and measured. Also measured was the signal in the comparison beam. Constancy of the signal from receiver 13 served as a criterion of the laser stability. We used MG-30 pyroelectric radiation receivers, whose signal was fed to selective microvoltmeters.

The accuracy with which the gap between the prism and the sample was maintained constant (when the prism was moved) was determined both by the accuracy with which the mechanism of the measuring pickup was manufactured (a "swallowtail" was used) and by the plane-parallelism of the glass plate on which the films were deposited. The optimum gaps (~50 μm under the input prism for the investigated copper samples and ~20 μm under the exit prism) were maintained accurate to ±5 μm. An increase of the distance between the prisms with the gaps kept constant caused an exponential decrease of the intensity of the radiation emerging from the exit prism. This made it possible to measure the

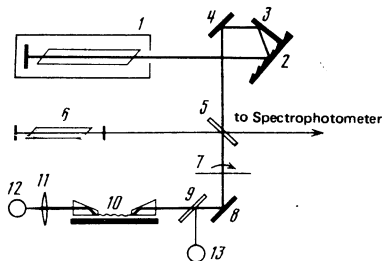


FIG. 1. Diagram of experimental setup.

path length and the absorption of the SEW.

The accuracy with which the SEW path length is determined depends on the precision of the mechanical units and of the signal measurements, as well as on the distance R by which the prisms are moved apart in the measurements. In our setup the accuracy of the measured SEW path length could be estimated from the formula

$$\Delta L/L \leq 0.15L/Rn^{1/2},$$

where n is the number of independent measurements of L . In the measurement presented usually $R > 2L$ and $n \geq 4$, and the accuracy of L was not worse than 4%.

The SEW path lengths were measured immediately after the deposition of the copper. It turned out that the SEW path length decreases with time, dropping by a factor 1.5 after a month. This cannot be attributed only to the formation of an oxide film, since the thickness of the natural oxide on the copper is usually ~30 Å, whereas the observed change in the SEW path length could be produced only by a film ~200 Å thick.¹² So large an increase in the absorption of the SEW can be explained by assuming that the oxygen in the air not only oxidizes the upper copper layer, thereby producing a film 30 Å thick, but also diffuses over the boundaries of the crystallites of the polycrystalline copper film, and this changes the optical constants of the copper below the surface layer. The calculation that agrees best with the experimental SEW path lengths in copper makes use of the parameters $\nu_p = 65\ 100\ \text{cm}^{-1}$ and $\nu_r = 430\ \text{cm}^{-1}$, if no account is taken of the oxide film. Allowance for a copper-oxide film 30 Å thick and with $\epsilon_3 = 7.3$ yields $\nu_r = 390\ \text{cm}^{-1}$ at the same plasma frequency. For copper with a silicon oxide film we took into account in the calculations the copper oxide film and used a collision frequency $\nu_r = 390\ \text{cm}^{-1}$.

The silicon oxide films were deposited only after the stabilization of the copper surface properties. The

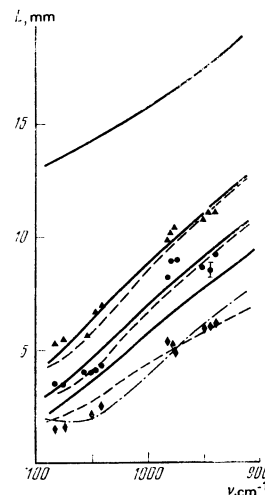


FIG. 2. Path length of SEW over the surface of copper with silicon-oxide film. Points—experimental values, curves—calculation using various models, whose parameters are listed in Table II: solid—model No. 1, dashed—model No. 2 for films 1 and 2 and model No. 3 for film 3, dash-dot—model No. 4. Upper curve—SEW path length over the surface of copper.

points of Fig. 2 show the measured path lengths in copper with silicon oxide films of three thicknesses, 120, 180 and 235 Å (the thickness measurement is described in the next section). In addition to the experimental points, Fig. 2 shows also the curves calculated by using various models. The comparison of the calculation and experiment is considered in greater detail in Sec. 5.

Just as in the preceding experiments,^{4,13} the measured frequency dependences of the SEW path length in the presence of silicon oxide films differ substantially from those calculated from the optical constants of silicon monoxide⁷ and silicon dioxide.¹⁴

In addition to the silicon oxide films we investigated also a natural oxide film on an aluminum surface, as well as the oxide film obtained by thermal oxidation on the surface of molybdenum. These experiments are described in greater detail in Sec. 6.

4. REFLECTION SPECTRA AND DETERMINATION OF FILM THICKNESSES

The limited spectral band containing the CO₂ laser lines (938–1080 cm⁻¹) prevented us from obtaining the complete contour of the band of SEW absorption by the silicon oxide film. To obtain additional information on the film we used the single-reflection spectra in the 800–1300 cm⁻¹ region, with the light incident on the sample at an angle ~70°. We used the MNPVO-1 attachment in which one of the mirrors and the IR spectrophotometer IKS-16 were replaced. The complications involved with placing the sample in the attachment (to replace the MNPVO element) and with the adjustment made exact quantitative measurements difficult. Moreover, it was impossible to measure reliably in this way the spectrum of the thinnest film 1 (the films are numbered in order of increasing thickness). The reflection spectra of the thicker films were obtained (Fig. 3) and used to determine the optical constants of the films together with the SEW spectra (see the next section).

To decrease the number of unknown film parameters, the thicknesses were determined ellipsometrically^{15,16} with the laser photoelectric ellipsometer LÉF-2 (He-Ne

TABLE I.

Sample No.	ψ_0 , deg	Δ_0 , deg	ψ , deg	Δ , deg	$\epsilon_{e'}$	$\epsilon_{e''}$	d_0 , Å	ϵ_2'	ϵ_2''	d , Å	ψ_{calc} , deg
1	44.24	129.52	44.30	116.81	-9.13	0.681	120	-12.10	0.944	120	44.30
2	44.32	130.39	44.43	111.86	-9.76	0.656	175	-12.76	0.896	180	44.42
3	44.27	129.54	44.53	106.67	-9.34	0.669	230	-12.21	0.944	235	44.44

laser, $\lambda = 6328$ Å). The angles measured were ψ and Δ , which characterize the ellipticity of the polarization of light reflected from the metal with the silicon oxide, and ψ_0 and Δ_0 obtained without the metal (Δ is the phase difference between the p and s polarization components of the light reflected from the sample, and $\tan\psi$ is the amplitude ratio). The angle of incidence of the light on the sample was 60°. The ellipsometry results are gathered in Table I, which lists also the calculated values of the complex permittivity of the copper and of the thickness of the silicon-oxide films.¹¹

For the system copper +SiO_x film with $\epsilon_2 = 3.5$ (ϵ_2 was determined on the basis of the proposed film composition discussed in the next section) a plot of Δ against thickness was constructed and used to determine the film thicknesses d_0 , which are also given in Table I. Allowance for the influence of the oxide film was made by calculating Δ_0 and ψ_0 for different values of the metal permittivity in the presence of the oxide film ($\epsilon_3 = 7.3$, $l = 30$ Å), while reconciliation of the calculated and experimental Δ_0 and ψ_0 yielded the value of ϵ_2 of copper with allowance for the oxide film. The thicknesses d of the silicon-oxide films were then determined just as without allowance for the oxide film. We note that the SiO_x thicknesses obtained with and without allowance for the oxide film on the copper differ insignificantly.

To check on the correctness of the determined thickness of film 3, this thickness was measured by interferometry using the Fizeau fringes.¹⁶ The shift of the multibeam interference fringes by the step formed by the film boundary was measured. The interferometer mirrors were an aluminum film covering the step and a semitransparent silver mirror. The shift of the fringes by the step was small, and we therefore photographed the interference pattern and determined the shift with a scanning microphotometer. The thickness obtained in this manner (235 ± 10 Å) agrees with that given in Table I.

5. OPTICAL CONSTANTS OF SILICON OXIDE FILMS

Calculations using the optical constants of silicon monoxide or dioxide do not agree with experiment. This confirms the assumed intermediate composition of the investigated films. To estimate the optical constants of the mixtures we used an approximation in which the refraction is assumed to be additive. It can be assumed that the SiO_x film consists of a mixture of silicon dioxide with permittivity ϵ_a (concentration $q = x - 1$) and silicon monoxide with permittivity ϵ_b (concentration $1 - q = 2 - x$); this model was used by Zolotarev.¹⁷ The permittivity of the mixture is calculated from the formula

$$\frac{\epsilon - 1}{\epsilon + 2} = q \frac{\epsilon_a - 1}{\epsilon_a + 2} + (1 - q) \frac{\epsilon_b - 1}{\epsilon_b + 2}. \quad (6)$$

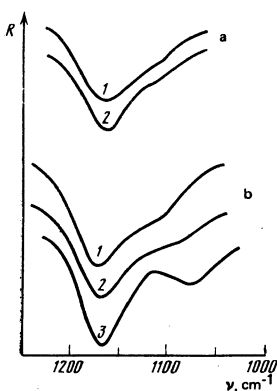


FIG. 3. Reflection spectra of SiO_x film on copper. Film thicknesses 180 Å (a) and 235 Å (b). Curves 1—experiment, remaining curves—calculation using various models, whose parameters are listed in Table II: 2a—model No. 1 for film 2, 2b—model No. 3 for film 3, 3b—model No. 4 for film 3.

The calculation yielded the concentration dependences of the transverse-oscillation frequencies (the maximum of the imaginary part of the permittivity) and of the longitudinal oscillations [the maximum of the loss function $\text{Im}(1/\epsilon)$]. These are plotted in Fig. 4. The permittivity of the silicon monoxide and dioxide were taken from Refs. 7 and 17. A plot similar to that shown in Fig. 4 is usually called two-mode.¹⁸ For $q \approx 0$ (or 1) the spectrum should contain the oscillations of the SiO (or SiO₂) and the local oscillation of the impurity. At intermediate concentrations we observed the oscillations of both SiO and SiO₂ with shifted frequencies. From these frequencies one can estimate the value of x corresponding to the longitudinal oscillation of frequency 1160 cm⁻¹ obtained from the reflection spectra (Fig. 3). We get $x = 1.2$, i.e., a mixture with 20% SiO₂ and 80% SiO. Calculation of the SEW and reflection spectra with this value of x does not lead to satisfactory agreement with experiment; this may be due to the fact that the refraction-additivity approximation does not hold in this case. The frequencies obtained in this manner were nevertheless used as the first approximation in the calculation of the optical constants of the SiO_x films.

To determine the optical constants of single crystals one frequently used a dispersion analysis (DA) of the reflection spectra.^{19, 20} We used DA of the spectra of the SEW and of the reflection from the films on the metal. The permittivity of the film and the metal was chosen in the so-called factorized form:¹⁹

$$\epsilon_z = \epsilon_\infty \prod_i \frac{\nu_{LOi}^2 - \nu^2 - i\gamma_i \nu}{\nu_{TOi}^2 - \nu^2 - i\gamma_i \nu} \quad (7)$$

with two oscillators. This formula is more convenient for DA than the customarily used formula with summation over the oscillators.¹⁹ The damping was assumed in Ref. 20 to be different for longitudinal oscillations (LO) (in the numerator) and the transverse oscillations (TO) (in the denominator), but we used equal values of the damping for the LO and TO oscillations.

The scheme of the DA was the following: The initial oscillator parameters were chosen and the frequency dependence of the SEW (or reflection) path length was calculated for a copper film, as well as the total deviation from the experiment. All the parameters were

varied next, and the direction of the gradient of the summary deviation was determined. A descent in the direction of the gradient was then made, until the minimum difference between calculation and experiment was reached.

For model SEW spectra, the DA analysis determines reliably the frequency of the longitudinal oscillation and the damping in the case when the SEW absorption band is in a measurable frequency interval. An ambiguity may arise if only one wing of the band is measured, while the maximum of the absorption and the other wing of the band are outside the measurable frequency region. To eliminate this ambiguity we used reflection spectra (Fig. 3) that made it possible to estimate the frequency of the longitudinal oscillation and the value of the damping. We found it difficult to carry out the DA of the reflection spectra because two parameters could not be determined accurately in our case: the incidence angle, owing to the large angular aperture of the beam incident on the sample (average value approximately 70°), and the level of the 100% reflection (the construction of the attachment was such that its adjustment could be upset when the samples were changed). The accuracy of the measurement of the SEW spectra was therefore higher than that of the measurement of the reflection spectra, the principal role was assumed by the DA of the SEW spectra, and the reflection spectra were used mainly to exclude errors due to the narrow spectral interval in which the SEW spectra were measured.

An ambiguity can arise in the DA of both the SEW spectra and in the reflection spectra because of the interdependence of the various parameters. Since the SEW absorption is proportional to the product of the film thickness by the loss function, and the latter is in turn proportional to the longitudinal-oscillator strength, it follows that

$$\alpha \sim l(\nu_{LO}^2 - \nu_{TO}^2). \quad (8)$$

The connection between the thickness and the frequency of the transverse oscillation does not make it possible to determine these two quantities simultaneously from the SEW spectrum (this situation is typical of optical thin films with thickness much smaller than the wavelength; for example, from the values of the reflection and of the transmission it is impossible to determine simultaneously the refractive index and the film thickness).

The results of the DA are summarized in Table II. Different versions of the model calculations are compared with experiment in Fig. 2. The solid curves (Fig. 2) were obtained using one and the same model (No. 1, Table II) for all three films. The agreement between the calculation and the experiment is good for films 1

TABLE II.

Model No.	ν_τ, cm^{-1}	$\nu_{TO1}, \text{cm}^{-1}$	$\nu_{LO1}, \text{cm}^{-1}$	ν_i, cm^{-1}	$\nu_{TO2}, \text{cm}^{-1}$	$\nu_{LO2}, \text{cm}^{-1}$	$\nu_\infty, \text{cm}^{-1}$	ϵ_∞
1	390	995	1115	100	1135	1160	60	3.3
2	390	980	1100	100	1132	1162	67	3.3
3	540	980	1100	100	1132	1162	67	3.3
4	390	915	1075	100	1125	1156	60	3.3

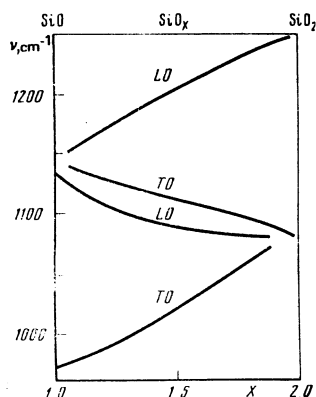


FIG. 4. SiO_x oscillation frequencies vs. composition. Calculation by Eq. (6).

and 2, but not for the thickest film. The agreement can be improved by taking film 3 to be 330 Å thick in place of the measured 235 Å. But so large a thickness difference is not very likely, and it must therefore be assumed that the optical constants of either the film or the metal have undergone a change. The increase of the absorption in film 3 is clearly seen in Fig. 5, which shows the dependence of the absorption coefficient on the film thickness. This dependence should be linear for the investigated thick films. Linearity is observed for three thicknesses 0, 120, and 180 Å; these points fit well a straight line. The absorption for the 235 Å thickness turned out to be much larger than calculated.

We have analyzed the two hypotheses advanced above concerning the causes of the deviation. To decrease the deviation, it can be assumed that all that was measured were the optical constants of the metal under film 3 compared with those prior to the deposition of the coating. This can result, for example, from the heating of the substrate when the silicon-oxide film is sputtered on, or from the contaminations contained in the evaporated (technical) silicon monoxide, since film 3 began to be coated first, was coated for a longer time, and was somewhat closer to the evaporator than the remaining films. The change of the optical constants of copper can be taken into account by increasing the electron collision frequency. The optical constants of the copper in the visible region should not be noticeably altered thereby, since the collision frequency is much lower than the frequency at which the measurements were performed. The contribution of the free electrons to the real part of the permittivity is well described by the Drude formula without allowance for the damping, and the imaginary part of the permittivity is much smaller than the real part and can receive a large contribution not only from the free electrons but also from interband transitions.

The DA analysis carried out assuming the permittivities of the films are additive and that only the electron collision frequencies in the copper are different allows us to select model 2 for films 1 and 2 and model 3 for film 3 (see Table II). The results of the calculation by these models is shown by the dashed lines of Fig. 2. The agreement with experiment for film 3 improved, but became somewhat worse for 1 and 2—the total difference between the experimental points and the calculation increased. This indicates that it is difficult to obtain good agreement by merely varying the substrate

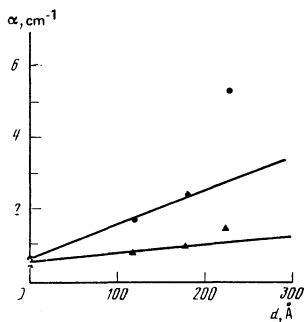


FIG. 5. SEW absorption vs. SiO_x film for 1050 cm^{-1} (●) and 943 cm^{-1} (▲).

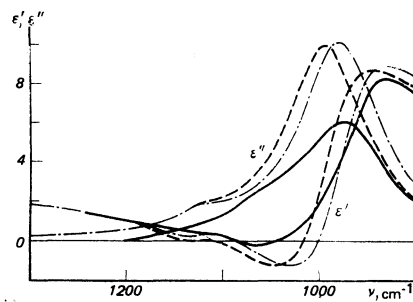


FIG. 6. Real (ϵ') and imaginary (ϵ'') parts of permittivity of silicon monoxide⁷ (solid curves) and of the SiO_x films investigated by us. Dashed curves—films 120 and 180 Å thick, thick, dash-dot curves—film 235 Å thick.

optical constant. It appears that the optical constants of the films must also be taken to be different.

If it is assumed that deposition of film 3 produced no changes whatever in the underlying copper, then the optical constants of this film should differ strongly from those of the two other films. The DA yields in this case the parameters of the oscillators of model 4 (Table II). The agreement of the experimental and calculated (dash-dot curve) SEW spectra is good, but the frequency of the transverse oscillation should be 915 cm^{-1} (in place of $980\text{--}1000 \text{ cm}^{-1}$). The shift, compared with silicon monoxide and compared with the model that assumes additivity of the refraction (Fig. 4), is very large.

It is possible to choose between models 3 and 4 for film 3 by using the reflection spectra (Fig. 3). Calculation by model 1 yields for the 180 Å film a spectrum (curve 2, Fig. 3a) close to the experimental one (curve 1, Fig. 3a). It is this agreement that can serve as the criterion for the choice. It is seen from Fig. 3b that the curve 2 calculated in accord with model 3 for a film 235 Å thick agrees well with the experimental curve, whereas for model No. 4 (curve 3) the deviation from experiment is very large: one can clearly see two minima in place of the experimental single asymmetric minimum.

The permittivities obtained by us for the silicon oxide films are shown in Fig. 6. The calculation was in accord with Eq. (10). For films 1 and 2 we used model No. 1 (dashed curves of Fig. 6), and for film 3 we used model No. 3 (dash-dot curve). For comparison we show also the permittivity of silicon monoxide (solid curves) obtained in Ref. 7 for much thicker films. The difference between the permittivity of film 3 from those of films 1 and 2 is not large, and the main contribution to the difference between the SEW spectra for these films is made by the change of the collision frequencies of the electrons in the copper.

6. SEW SPECTRA AND OPTICAL CONSTANTS OF THE NATURAL OXIDE FILM ON ALUMINUM AND OF THE OXIDE FILM THERMALLY PRODUCED ON MOLYBDENUM

Our measurements of the SEW path length over the surface of aluminum in air have shown a distinct deviation from the frequency dependence for the pure metal,

due to the selective absorption in the natural oxide film. Using the same laser frequencies as in the measurements described above, we were unable to obtain the contour of the SEW absorption line, since the absorption maximum 940 cm^{-1} was at the edge of the operating band of the $^{12}\text{C}^{16}\text{O}_2$ laser lines. The use of the carbon isotope ^{13}C permits extension of the frequency band. We used a laser with a mixture of $^{13}\text{C}^{16}\text{O}_2$ and $^{12}\text{C}^{16}\text{O}_2$, which permitted operation at frequencies from 868 to 1080 cm^{-1} . The frequency dependence of the SEW path length over the aluminum surface is shown in Fig. 7. From the spectrum it is possible to determine the frequency of the longitudinal oscillations of the oxide film, $\nu_{LO} = 940\text{ cm}^{-1}$, and the width of the absorption band, $\gamma \approx 50\text{ cm}^{-1}$. The obtained frequency is close to the natural-oxide frequencies measured by using multiple reflection²¹ and by the photoacoustic method.²²

A single-oscillator model was used in the calculations. The two parameters of the oscillator (ν_{LO} , γ) were already given above. The high-frequency permittivity was assumed to be $\epsilon_\infty = 3$ (Ref. 23); the frequency of the transverse oscillations was $\nu_{TO} \approx 650\text{ cm}^{-1}$ (according to measurements²⁴ performed for thicker anodized films). We used for aluminum a plasma frequency $\nu_p = 94000\text{ cm}^{-1}$, while the conduction-electron collision was estimated from approximate formulas to be 840 cm^{-1} and was varied in the calculations. The plasma frequency was measured by a procedure described elsewhere,²⁵ where the optical constants of copper were determined.

In the investigation of the silicon-oxide films we measured the thickness by an independent method; this facilitated the determination of the film optical constants. The published values of the thicknesses of natural oxide films on aluminum vary and range from 15 \AA (for dry air) to $30\text{--}40\text{ \AA}$ (for humid air). The frequency of the transverse oscillations for the thicker films was already indicated above. The dispersion analysis of the frequency dependence of the SEW path length led to an expected result. If the film thickness is assumed to be 20 \AA , then the frequency of the transverse oscillations should be greatly changed: the DA yields 890 cm^{-1} instead of 650 cm^{-1} . If it is assumed that the frequencies of the transverse oscillations agree with the published values for thick oxide films, the calculated film thickness should be $\sim 5\text{ \AA}$, a very low value for a natural oxide film.

To explain the results it can be assumed either that a homogeneous oxide film 20 \AA thick has a transverse-

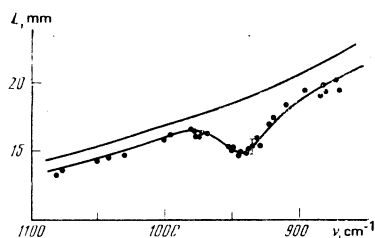


FIG. 7. Calculation of frequency dependence of path length of SEW over aluminum without oxide (upper curve) and with oxide film 15 \AA thick (lower curve). Points—experiment. The permittivity of the oxide film is shown in Fig. 8.

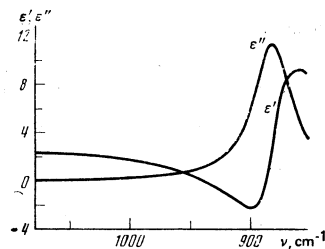


FIG. 8. Effective permittivity of natural layer of aluminum oxide.

phonon frequency that differs greatly from that of the thicker anodized oxide films on aluminum at approximately the same frequency of the longitudinal oscillations (the permittivity of such a layer, obtained from a DA of the SEW spectrum, is shown in Fig. 8), or else that the oxide layer is inhomogeneous, and then different methods of measuring its thickness will give different values. The effective film thickness determined from the SEW absorption is $\sim 5\text{ \AA}$. This would mean that the pure aluminum oxide is located only on the surface (a monomolecular layer would be $\sim 3.7\text{ \AA}$ thick), and beneath it is a transition layer in which the oxide is mixed with aluminum; the component concentrations and the optical constants of the layer vary with depth. In this case the permittivity shown in Fig. 8 can be regarded only as the effective permittivity of an inhomogeneous oxide layer. If the free carriers screen the Coulomb interaction in the transition layer, thereby decreasing the oscillator strength, then the transition layer produces no selective absorption in the SEW spectra. Calculation of the SEW spectrum for the "aluminum + conducting transition layer + aluminum oxide system having the optical constants of thick films" has shown that by varying the conductivity and the thickness of the transition layer ($\sim 20\text{ \AA}$) and the thickness of the oxide layer ($\sim 5\text{ \AA}$), and also by varying the conductivity of the aluminum, it is possible to obtain fair agreement with experiment, but a similar macroscopic calculation for a practically monomolecular film must apparently be regarded only as a qualitative confirmation of the possibility of using the proposed model.

In contrast to aluminum and copper, molybdenum is stable at room temperature to the action of the oxygen in the air. Oxidation starts only when the temperature is raised to 250°C in a humid atmosphere or to 400°C in a dry atmosphere.²⁶ Growth of an oxide film on molybdenum at temperature 397°C and higher was detected in Ref. 27 by using infrared radiation. An oxide film 380 \AA thick is produced within approximately one hour. Using the high sensitivity of the SEW spectroscopy, we investigated the earlier stages of oxide growth on molybdenum. The samples were prepared by annealing molybdenum foil in an oven. At a temperature as low as 220°C an oxide film is formed after 10 minutes, as revealed by the SEW absorption. The frequency dependence of the SEW free path of this sample is shown in Fig. 9 (curve 2). The upper curve 1 is the SEW spectrum of the molybdenum foil prior to annealing. Curve 3 is the SEW spectrum of the molybdenum oxide produced after 35 minutes of oxidation at 310°C . The ap-

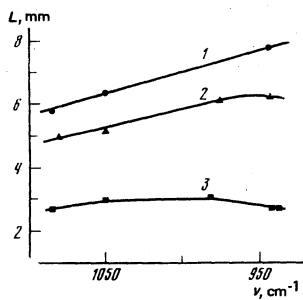


FIG. 9. Experimental frequency dependence of path length of SEW over molybdenum prior to annealing (curve 1) and after annealing (curves 2 and 3).

pearance of the selective absorption band of the molybdenum oxide after heating is clearly seen. The thicknesses of the oxide films, obtained from the DA of the SEW spectrum, amount to 35 Å (for curve 2) and 210 Å (for curve 3). It was assumed in the calculations that the frequency of the transverse oscillation of the film is $\nu_{TO} \approx 800 \text{ cm}^{-1}$ (the same as for molybdates), $\nu_{LO} = 950 \text{ cm}^{-1}$, $\epsilon_{\infty} \approx 3$, and $\nu_p = 40\,000 \text{ cm}^{-1}$ (the plasma frequency of molybdenum).

CONCLUSION

A joint DA of the SEW and reflection spectra at large incidence angles has yielded the damping frequencies of the optical oscillations in silicon-oxide films deposited on the surface of copper, as well as the frequency dependence of the permittivity of the films. For two silicon-oxide films 120 and 180 Å thick we observed no difference in the spectra and the optical constants. For the 235 Å film a small change in the optical constant of the silicon oxide is observed compared with the thinner films, as well as a noticeable change of the optical constants in the surface layer of the copper under the film.

A high sensitivity of SEW spectroscopy was realized in an investigation of a natural oxide film on the surface of aluminum and of a thermally grown oxide film on molybdenum. The SEW absorption spectrum of the aluminum-oxide film points to a noticeable difference between the properties of the natural-oxide film from those obtained by others for thicker (anodized) films. It can be assumed that a considerable fraction of the thickness of such a thin film constitutes a transition layer consisting of a mixture of the oxide with pure aluminum.

¹⁾In the first-approximation calculation it was assumed that the copper surface is not oxidized; the permittivity ϵ_{40} of copper was calculated. The permittivities of the copper differ little in the three copper films, possibly in connection with the distribution of the flux of copper atoms evaporated from the vessel (as indicated above, these difference are insignificant in the IR region).

- ¹J. Schoenwald, E. Burstein, and F. M. Elson, *Sol. State Commun.* **42**, 185 (1973).
- ²V. M. Agranovich and V. L. Ginzburg, *Kristaloptika s uchetom prostranstvennoi dispersii i teoriya éksitonov* (Spatial Dispersion in Crystal Optics and the Theory of Excitons), Nauka, 1979 [Wiley, 1967].
- ³R. J. Bell, R. W. Alexander, C. A. Ward, and J. L. Tyler, *Surface Sci.* **48**, 253 (1975).
- ⁴G. N. Zhizhin, M. A. Moskaleva, E. G. Shomina, and V. A. Yakovlev, *Pis'ma Zh. Eksp. Teor. Fiz.* **24**, 221 (1976) [*JETP Lett.* **24**, 196 (1976)].
- ⁵K. Bhasin, D. Bryan, R. W. Alexander, and R. J. Bell, *J. Chem. Phys.* **64**, 5019 (1976).
- ⁶G. N. Zhizhin, N. N. Morozov, M. A. Moskaleva, A. A. Sigarev, E. V. Shomina, V. A. Yakovlev, and V. M. Grigos, *Opt. Spektrosk.* **48**, 181 (1980) [*Opt. Spectrosc.* **48**, 102 (1980)].
- ⁷F. T. Cox, G. Hass, and W. R. Hunter, *Appl. Opt.* **14**, 1247 (1975).
- ⁸C. A. Ward, K. Bhasin, R. J. Bell, R. Alexander, and J. Tyler, *J. Chem. Phys.* **62**, 1674 (1975).
- ⁹R. G. Greenler, *ibid.* **55**, 310 (1966); **50**, 1963 (1969).
- ¹⁰in: *Physics of Thin Films: Advances in Research and Development*, Academic, Vol. 4 [Russ. transl. Mir, 1970, p. 334].
- ¹¹G. N. Zhizhin, M. A. Moskaleva, E. V. Shomina, and V. A. Yakovlev, *Pis'ma Zh. Eksp. Teor. Fiz.* **29**, 533 (1979) [*JETP Lett.* **29**, 486 (1979)].
- ¹²D. A. Bryan, D. L. Begley, K. Bhasin, R. W. Alexander, and R. J. Bell, *Surface Science* **57**, 53 (1976).
- ¹³G. N. Zhizhi, M. A. Moskaleva, E. V. Shomina and V. A. Yakovlev, in: *Teoreticheskaya spektroskopiya* (Theoretical Spectroscopy), Nauka, 1977, p. 243.
- ¹⁴V. M. Zolotarev, *Opt. Spekt.* **29**, 66 (1970).
- ¹⁵L. V. Semenenko, K. K. Svitashv, and A. I. Semenenko, in: *Nekotorye problemy fiziki i khimii poverkhnosti poluprovodnikov* (Some Problems in the Physics and Chemistry of Semiconductor Surfaces), Novosibirsk, Nauka, 1972, p. 114.
- ¹⁶R. Glang, in: *Handbook of Thin Film Technology*, L. Maissel and R. Glang, eds., McGraw, 1970 [Russ. transl., Sov. Radio, 1977, Vol. 1, p. 9].
- ¹⁷V. M. Zolotarev, *Zh. Prikl. Spektrosk.* **17**, 1052 (1972).
- ¹⁸E. A. Vinogradov and L. N. Vodop'yanov, *Fiz. Tverd. Tela* (Leningrad) **17**, 3161 (1975) [*Sov. Phys. Solid State* **17**, 2088 (1975)].
- ¹⁹V. A. Spitzer and D. N. Kleinman, *Phys. Rev.* **121**, 1324 (1961).
- ²⁰F. Gerwais and B. Piriou, *J. Phys.* **C7**, 2374 (1974).
- ²¹F. P. Mertens, *Surface Sci.* **71**, 161 (1978).
- ²²P. E. Nordal and S. O. Kanstad, *Optics Commun.* **24**, 95 (1978).
- ²³L. Harris, *J. Opt. Soc. Am.* **45**, 27 (1955).
- ²⁴A. J. Maeland, R. Rittenhouse, W. Lahar, and P. V. Romano, *Thin Solid Films* **21**, 67 (1974).
- ²⁵G. N. Zhizhin, M. A. Moskaleva, E. V. Shomina, and V. A. Yakovlev, *Fiz. Tverd. Tela* (Leningrad) **21**, 2828 (1978) [*Sov. Phys. Solid State* **21**, 1630 (1978)].
- ²⁶M. A. Lebedinskii, *Élektrovakuumnye materialy, metalli i splavy* (Electro-vacuum Materials, Metals and Alloys), Energiya, 1966.
- ²⁷L. M. Gratton, S. Paglia, F. Scattaglia, and M. Cavallini, *Appl. Spectr.* **32**, 210 (1978).

Translated by J. G. Adashko